ELSEVIER

International Journal of Solids and Structures 40 (2003) 7385–7397

INTERNATIONAL JOURNAL OF SOLIDS and STRUCTURES

www.elsevier.com/locate/ijsolstr

Investigations to the effect of heating-rate on the mechanical properties of aluminum alloy LY12 ☆

X. Peng [a,*], J. Fan [a], Y. Yang [a], Y. Chen [b], Y. Yin [b]

[a] *Department of Engineering Mechanics, Chongqing University, Chongqing 400044, China*
[b] *Academy of Engineering Physics of China, Chengdu 610003, China*

Received 26 March 2003; received in revised form 16 August 2003

Abstract

Two classes of experiments were conducted with a Gleeble 1500 thermal–mechanical testing system to investigate the effect of heating-rate and its history on the mechanical behavior of aluminum alloy LY12. In the first class of experiment, specimens were heated at different heating-rates to prescribed temperatures and then stretched until fracture. It was found that the specimen heated with higher heating-rate possesses lower rupture strength. In the second class of experiment, the specimens were preloaded and then heated at different rates until fracture. It was found that the higher the heating-rate was, the lower the failure temperature would be. Metallographical analysis showed that there are more defects in the specimens undergoing higher heating-rate. It was conjectured that higher heating-rate may cause stronger local thermal inconsistency due to the heterogeneous nature of the material. It may then cause local residual microstress fields, which, together with external thermal–mechanical load, may result in the changes in the microstructure of the material, such as recovery, recrystallization, nucleation and growth of microdefects, accounting for the changes in the macroscopic mechanical properties including hardening/softening, damage and failure, etc. A numerical simulation was performed, in which the mechanisms of local thermal inconsistency and the effect of the influencing factors were investigated.

Keywords: Aluminum alloy; Heating rate; Mechanical properties; Local thermal inconsistency

1. Introduction

The failure of materials and structures caused by the deposition of highly concentrated energy is receiving increasing attention (Chen et al., 1992, 1995, 2001; Chen and Li, 1992; Li and Chen, 1994; Chen, 1997; Liu et al., 1995, 1996; Wang et al., 1995; Han et al., 1999). A significant phenomenon is that the high and rapid increasing temperature generated by highly concentrated energy deposition may result in a remarkable change of the mechanical properties of materials. It may cause the failure of a preloaded structure

☆ Financial supported by NSFC (19272119) and the Education Ministry of China.
* Corresponding author. Tel.: +86-23-6510-3755; fax: +86-23-6510-6656.
E-mail address: xhpeng@cqu.edu.cn (X. Peng).

0020-7683/$ - see front matter © 2003 Elsevier Ltd. All rights reserved.
doi:10.1016/j.ijsolstr.2003.08.016

due to the degradation of the mechanical properties (e.g., the strength is reduced to below the applied stress), or the invalidation of the designed functions due to the redistribution of stress and the changes of configuration. The study on the material degradation at high and rapid increasing temperature may, on one hand, help avoiding such kind of failure, and on the other hand, provide available information for making use of fast-heating technology. The effect of elevated temperature on the mechanical properties of materials has been studied extensively, but less attention has been paid to the effect of heating-rate.

It was observed that fast heating could cause distinct change in the mechanical properties of aluminum alloy LY12 (Liu et al., 1995). When investigating the nonlinear softening of aluminum alloy and brass subjected to fast heating, it was found that the difference in heating-rate history may cause differences in both the grain size and the macroscopic mechanical properties, which was accounted for with the dynamics of recrystallization (Liu et al., 1995). The tensile testing of low-alloy steel 30CrMnSi subjected to fast-heating histories with different heating-rates showed distinct difference in both the rupture strength and the metallograph of the material (Wang et al., 1995). The experimental investigation to the effect of heating-rate on the mechanical properties of preloaded brass H62 indicated that the failure temperature reduces with the increase of heating-rate, which was attributed to the increase of microdefects due to the strong local thermal inconsistency at high heating-rate (Chen et al., 2001).

In this paper, a systematic experiment was conducted with a Gleeble 1500 thermal–mechanical material testing system to investigate the effect of heating-rate history on the rupture strength of aluminum alloy LY12, and the effect of heating-rate on the failure temperature of pre-loaded LY12 specimens. The metallographs of the tested material were observed and analyzed to investigate the mechanisms of the effect of heating-rate. It is conjectured that the local thermal inconsistency (LTI) due to the inevitable heterogeneity and the nonhomogeneous nature of the material may play an important role in the damage and failure of the material. A numerical simulation was performed, which showed that the additional stress caused by high heating rate could increase remarkably even at a very low temperature.

2. Experiment

2.1. Experimental conditions

In order to investigate the effect of heating-rate history on the rupture strength of aluminum alloy LY12 and the effect of heating-rate on the failure temperature of the preloaded LY12 specimens, two classes of experiments were performed, respectively, with a Gleeble 1500 thermal–mechanical material testing system. In both classes of experiments, the specimens were heated with direct current by applying an electrical voltage directly between the two ends of a specimen. During an experiment, the temperature and its rate were measured with a chromel–alumel thermocouple welded directly on the surface of the working section and controlled by a computer. The elongation of a specimen, the tensile traction and the temperature were recorded synchronously with the data acquisition element of the testing system. The material used for testing is aluminum alloy LY12, with the composition listed in Table 1. The solidus and the melting temperatures of LY12 are about 530 and 650 °C, respectively. The geometry of the specimen is shown in Fig. 1, where a reedy working section is used for larger electric resistance to meet the requirement of high heating-rate and uniform distribution of temperature in the working section. The simulation for the

Table 1
Composition of the aluminum alloy LY12 (%)

Cu	Mg	Mn	Fe	Si	Al
4.4	1.6	0.6	0.4	0.4	Rest

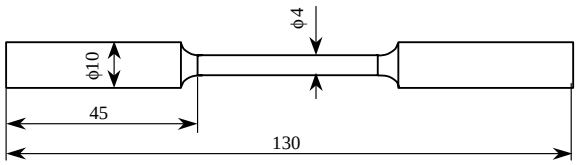

Fig. 1. Geometry of specimen.

temperature distributions generated by different electrical voltages with a finite element approach showed sufficiently uniform distributions of temperature in the working section of the specimen at different moments during the working period, provided the diameter of the working section keeps uniform.

In the first class of experiment, the effect of heating-rate history on the rupture strength of aluminum alloy LY12 was to be investigated. It includes three steps: heating a specimen at a constant heating-rate to the prescribed temperature; and then keeping the temperature unchanged for 1 s followed by stretching the specimen until fracture. The second step was used to make the temperature uniform without introducing distinct changes in the metallographic structure of the material. In the third step, the strain rate was fixed as $0.5\ s^{-1}$, so that the total time interval of this step could be less than 0.1 s.

In the second class of experiment, the effect of heating-rate on the failure temperature of preloaded LY12 specimens was to be investigated. It includes two steps: (1) stretching a specimen to a prescribed tensile stress; and (2) heating the specimen at a prescribed heating-rate, while keeping the preloaded stress unchanged, until fracture. However, it could be imagined that, with increasing temperature, the specimen might gradually lose the capability of bearing the preloaded stress due to the softening of the material at elevated temperature. The failure temperature can, therefore, be defined as the temperature at which the prescribed preloaded stress can no longer be held (or falls distinctly), which indicates that the specimen has lost the load-bearing capability to the prescribed preloaded stress at this temperature.

2.2. Effect of heating-rate history on the rupture strength of LY12

The conditions used for the investigation to the effect of heating-rate history on the rupture strength of LY12 are shown in Table 2. Three final working temperatures, 100, 350 and 495 °C, were prescribed and heating-rates 200, 600 and 1000 °C/s were employed for each working temperature, respectively. The working temperature ranges from near room temperature to near solidus temperature (530 °C). The maximum heating-rate is determined by the capability of the testing system and the geometry of specimen and the properties of the used material. Three specimens were used for each testing condition.

The load–elongation curves of LY12 specimens under the conditions given in Table 2 are shown in Fig. 2. It can be seen that, in general, the load-bearing capability is reduced with the increase of working temperature due to temperature induced softening. At lower temperature, heating-rate history does not distinctly affect the load-bearing capability of the specimen, but the effect becomes remarkable at higher temperature.

Table 2
Conditions for the first class of experiment

Heating-rate dT/dt (°C/s)	Final temperature T (°C)		
	100	350	495
200	A-200	B-200	C-200
600	A-600	B-600	C-600
1000	A-1000	B-1000	C-1000

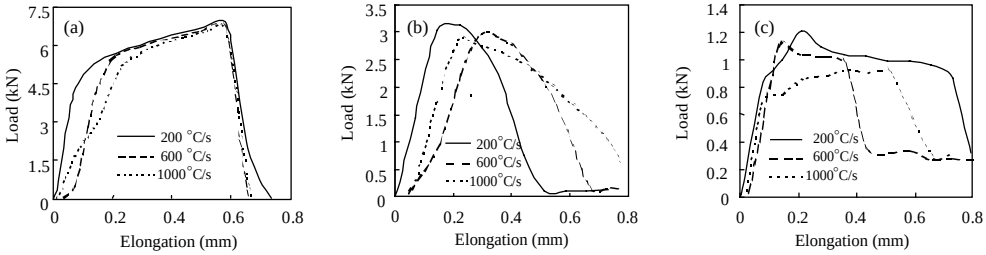

Fig. 2. Load–elongation curves of LY12 specimens at different temperatures and subjected to different heating-rate histories. (a) $T = 100$ °C, (b) $T = 350$ °C, (c) $T = 495$ °C.

The rupture strength against heating-rate at different temperatures is shown in Fig. 3. It can be seen that at $T = 100$ °C, the rupture strength corresponding to different heating-rate histories do not show marked difference, except that at the heating-rate of 600 °C/s the rupture strength is slightly higher than that at the other two heating-rates. At both $T = 350$ and 495 °C, the rupture strength decreases with the increase of heating-rate.

Fig. 4 shows the variation of contraction ratio of the cross section ψ at different temperatures against heating-rate. At working temperature $T = 100$ °C, the effect of heating-rate is negligible because of the very low working temperature and very short heating time. At $T = 350$ °C, ψ is much higher than that at the other two working temperatures, which could be attributed to the increase of ductility of the material due to recrystallization at elevated temperature. At $T = 495$ °C, ψ seems much smaller than that at $T = 350$ °C, and decreases with the increase of heating-rate. The former could be accounted for by the growth of grain

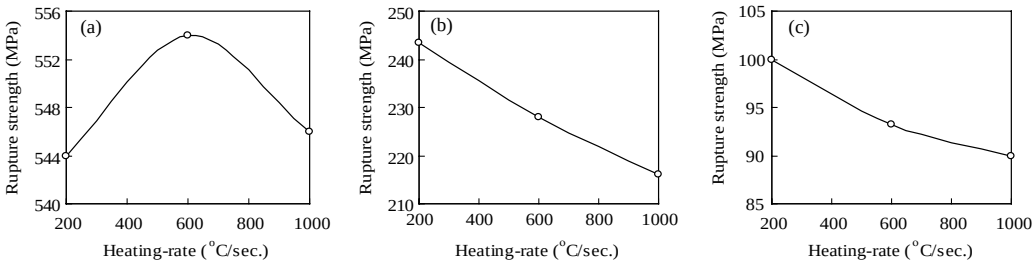

Fig. 3. Variation of rupture strength vs. heating-rate history at different temperatures. (a) $T = 100$ °C, (b) $T = 350$ °C, (c) $T = 495$ °C.

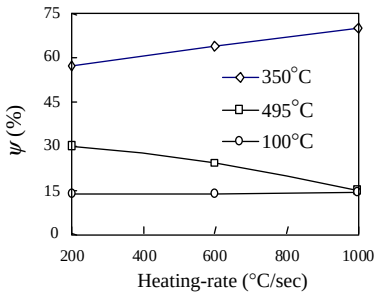

Fig. 4. Variation of contraction ratio of cross section ψ vs. heating-rate history at different temperatures.

Table 3
σ_f and ψ under different testing conditions

	Testing group									
	A-200	A-600	A-1000	B-200	B-600	B-1000	C-200	C-600	C-1000	RT
σ_f (MPa)	544	554	546	243	228	216	100	93	90	540
ψ (%)	13.7	13.8	14.3	57.5	63.9	69.9	30.4	24.3	15.2	13.5

RT: room temperature.

and the weakening of grain boundary at high temperature, while the latter could be attributed to the damage caused by local thermal inconsistency at very high heating rate, which will be discussed later. The observation to the break section shows that the fracture is ductile at $T = 350$ °C, but brittle at both $T = 100$ and 495 °C, which is consistent with the results shown in Fig. 4. Table 3 shows the rupture strength σ_f and contraction ratio of cross section of LY12 under the testing conditions given in Table 2, the data shown in Table 3 is the mean of testing results of the three specimens in each group. The rupture strength and contraction ratio of cross section at room temperature is also given in the last column of Table 3 for comparison.

2.3. Effect of heating-rate on the failure temperature of preloaded LY12 specimens

The conditions used to investigate the effect of heating-rate on the failure temperature of preloaded LY12 specimens are shown in Table 4. Four levels of preloaded stress, 105, 135, 165 and 195 MPa, were prescribed, for each of which three different heating-rates, 200, 600 and 1000 °C/s, were assigned. A specimen was preloaded to a prescribed stress level before heated with one of the three prescribed heating-rates. It could be imagined that the specimen would lose its capability of bearing the prescribed preloaded traction at some temperature due to softening, and then be elongated quickly until fracture.

Fig. 5 shows the measured relationships between temperature and time, stress and temperature, and strain and temperature, respectively, of the specimens subjected to the condition D-200 (Table 4). It can be seen that the temperature increases almost linearly at the rate of 200 °C/s (Fig. 5(a)). The prescribed preloaded stress $\sigma_0 = 195$ MPa almost maintains until some critical temperature is reached, then it falls rapidly (Fig. 5(b)). As previously defined, this critical temperature is the failure temperature corresponding to the given testing condition, at which the specimen can no longer keep its original load-bearing capability. The variation of stress against temperature shown in Fig. 5(b) is consistent with the phenomenon shown in Fig. 5(c), where strain develops at a smaller slope when the temperature is below the failure temperature, but it develops much faster when the temperature gets over the critical value.

Fig. 6 shows the measured results under the condition D-1000 (Table 4). The variations of temperature against time, preloaded stress against temperature, and strain against temperature show similar tendencies as shown in Fig. 5, although the heating-rate is much higher. However, compared with the results for the

Table 4
Experimental conditions for testing the failure temperature of preloaded LY12 specimens

Pre-loaded stress σ_0 (MPa)	Heating-rate		
	200 (°C/s)	600 (°C/s)	1000 (°C/s)
105	A-200	A-600	A-1000
135	B-200	B-600	B-1000
165	C-200	C-600	C-1000
195	D-200	D-600	D-1000

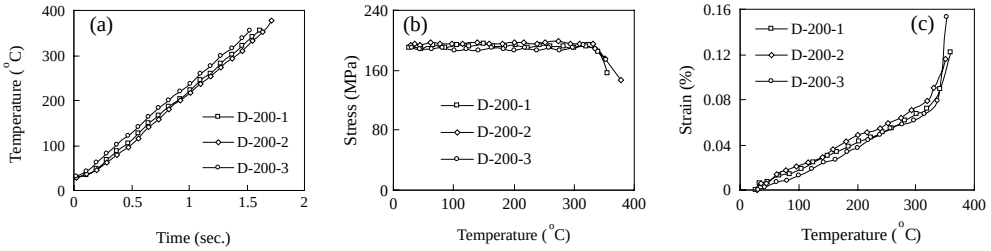

Fig. 5. Experimental results corresponding to D-200. (a) Temperature vs. time, (b) stress vs. temperature, (c) strain vs. temperature.

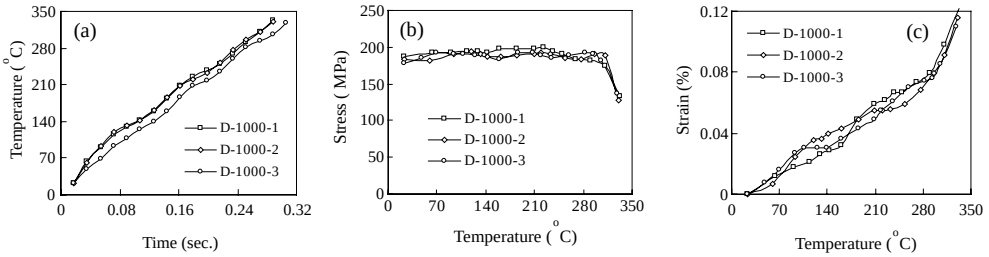

Fig. 6. Experimental results corresponding to D-1000. (a) Temperature vs. time, (b) stress vs. temperature, (c) strain vs. temperature.

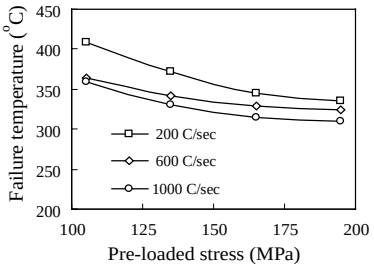

Fig. 7. Variation of failure temperature against preloaded stress.

condition D-200, it can be seen that the failure temperature corresponding to D-1000 is distinctly lower, though the preloaded stress is identical.

Fig. 7 shows the variation of failure temperature against the preloaded stress, taking heating-rate as a parameter. It can be seen that, for a fixed heating-rate, the failure temperature of the pre-loaded material reduces with the increase of pre-loaded stress, due to the softening of material at elevated temperature. In general, higher heating-rate results in lower failure temperature.

The variation of failure temperature against heating-rate at different pre-loaded stress is shown in Fig. 8. Remarkable reduction in failure temperature can be observed with the increase of heating-rate, which implies that heating-rate may play a significant role in the failure of the pre-loaded material. Especially, in the case of high level of preloaded stress, the difference between the failure temperatures tends to be negligible, and the effect of heating-rate becomes dominant, as can be observed by comparing the curves corresponding to $\sigma_0 = 165$ and 195 MPa (Fig. 5).

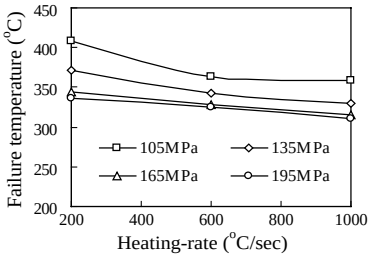

Fig. 8. Variation of failure temperature against heating rate.

2.4. Metallographic observation and analysis

It is known that, when subjected to thermomechanical loading, the change of the mechanical properties of materials is closely related to the microstructure of the material and its variation. For example, dislocation substructure, damage, recovery, recrystallization at certain stress and temperature, growth of grains and weakness of grain boundary, etc., may strongly influence the mechanical properties as well as the failure mode of a material. In order to make clear the mechanisms of the effect of heating-rate and its history on the mechanical properties of LY12, the metallographs of the deformed material were observed and analyzed. The samples used for the metallographical observation were cut from the vicinity of the fracture section of tested specimens, eroded in a mixed 2.5%HNO_3, 1.5%HCl and 1%HF solution for 10–20 s, and then cleaned for observation.

Before analyzing the mechanism of the effect of heating-rate on the mechanical properties of materials, we like to introduce briefly the concept of LTI. It is known that most engineering materials are, in nature, heterogeneous. The inhomogeneous nature of the microstructure, such as heterogeneity, grains with different orientations, grain boundaries and phase boundaries, dislocations and dislocation substructures, and inclusions, gives rise to the difference in the physical, thermal and mechanical properties in different material elements, such as thermal and electrical conductivity, specific heat, and thermal expansion coefficient, etc. It may cause LTI, i.e., nonuniform distribution of local temperature, and local residual stress distribution during a fast-heating process. For example, when a material is heated with a large electrical current, the difference in the electrical and thermal properties between local elements may result in a nonuniform distribution of local temperature. It, in turn, results in additional local residual stress, besides the conventional macroscopic residual thermal stress. The important is that, if the heating-rate is sufficiently large during a fast-heating process, the induced additional local residual stress may result in complicated changes in the mechanical properties of the material. Moderate local residual stress may cause hardening, contributing to an improvement of the mechanical property. At a sufficiently large heating-rate, the induced severe LTI may result in very high local temperature and local residual stress. The former may induce local softening, and the latter may cause local damage, which may degrade the mechanical properties of material and make the material fail even at a low level of preloaded stress.

Fig. 9(a)–(c) shows the metallographs of the material near the fracture sections of the specimens subjected to preloaded stress $\sigma_0 = 105$ MPa and heating-rates of 200, 600 and 1000 °C/s, respectively. Marked difference can be found in the metallographs corresponding to different heating-rates. At lower heating-rate, less and smaller defects are observed, which are mainly small voids. The corresponding change in the material properties is mainly determined by the temperature-induced change in the microstructure of the material, such as temperature induced softening, the possible recrystallization at medium temperature and growth of grain at high temperature. The deformation is almost uniform and the effect of LTI is unconspicuous. With the increase of heating-rate, defects develop in both density and size. It can be attributed to

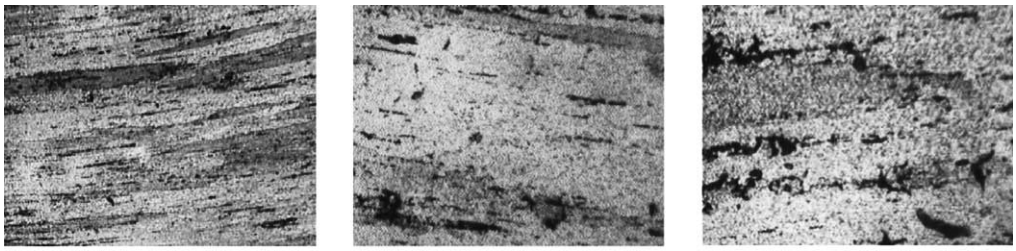

Fig. 9. Metallographs near the fracture portion of specimen subjected to $\sigma_0 = 105$ MPa (100×). (a) 200 °C/s, (b) 600 °C/s, (c) 1000 °C/s.

the enhancement of LTI, which enhances the local residual stress and, in turn, expedites the nucleation, growth and the coalescence of defects. At high heating-rate, severe LTI can even result in very high local temperature and severe local residual stress, together with the applied preloaded stress, accounting for the large amount of cracks and the brittle fracture of the specimens. No distinct recrystallization could be observed in the three cases shown in Fig. 9, which may be attributed to the low level of applied preloaded stress that is not sufficiently large to induce distinct recrystallization in a short time.

Fig. 10(a)–(c) shows the metallographs near the fracture sections of specimens subjected to preloaded stress $\sigma_0 = 165$ MPa and heating-rates 200, 600 and 1000 °C/s, respectively. Distinct recrystallization can be observed in Fig. 10(a), which can be accounted for with the higher applied stress and longer heating time due to the low heating-rate. Recrystallization can be also found in Fig. 10(b), but it is not so sufficient as in Fig. 10(a) due to the relatively shorter heating time interval. Compared with Fig. 9(a) and (b), less defects or cracks can be found in Fig. 10(a) and (b) although the testing conditions are similar except the larger preloaded stress that assists the recrystallization. Recrystallization can reduce, to some extent, the plastic deformation induced substructures and hardening, microdefects, and as the result, enables the material to endure more plastic deformation. Fig. 10(c) corresponds to the heating-rate of 1000 °C/s, in which plenty of cracks and defects can be observed, which is due to severe LTI and high level of the applied stress, and insufficient recrystallization because of the very short heating time interval.

A common characteristic in Figs. 9 and 10 is that, the defects in the material increase remarkably with the increase of heating-rate. Comparison between the metallographs of the material subjected to identical heating-rate but different preloaded stress, $\sigma_0 = 105$ and 165 MPa, shows less defects in the material with $\sigma_0 = 165$ MPa, which can be accounted for by the more adequate recrystallization at this applied stress.

The metallographs near the fracture section of the tensile specimens, tested at $T_f = 100$, 350 and 495 °C and heated with $dT/dt = 200$ and 1000 °C/s (referred to Table 2), are shown in Fig. 11, respectively. It

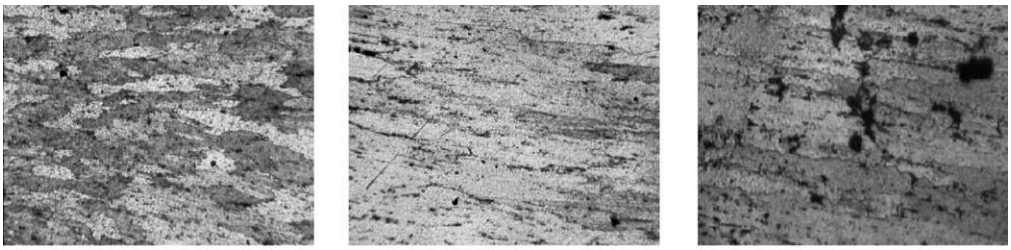

Fig. 10. Metallographs near the fracture portion of specimen subjected to $\sigma_0 = 165$ MPa (100×). (a) 200 °C/s, (b) 600 °C/s, (c) 1000 °C/s.

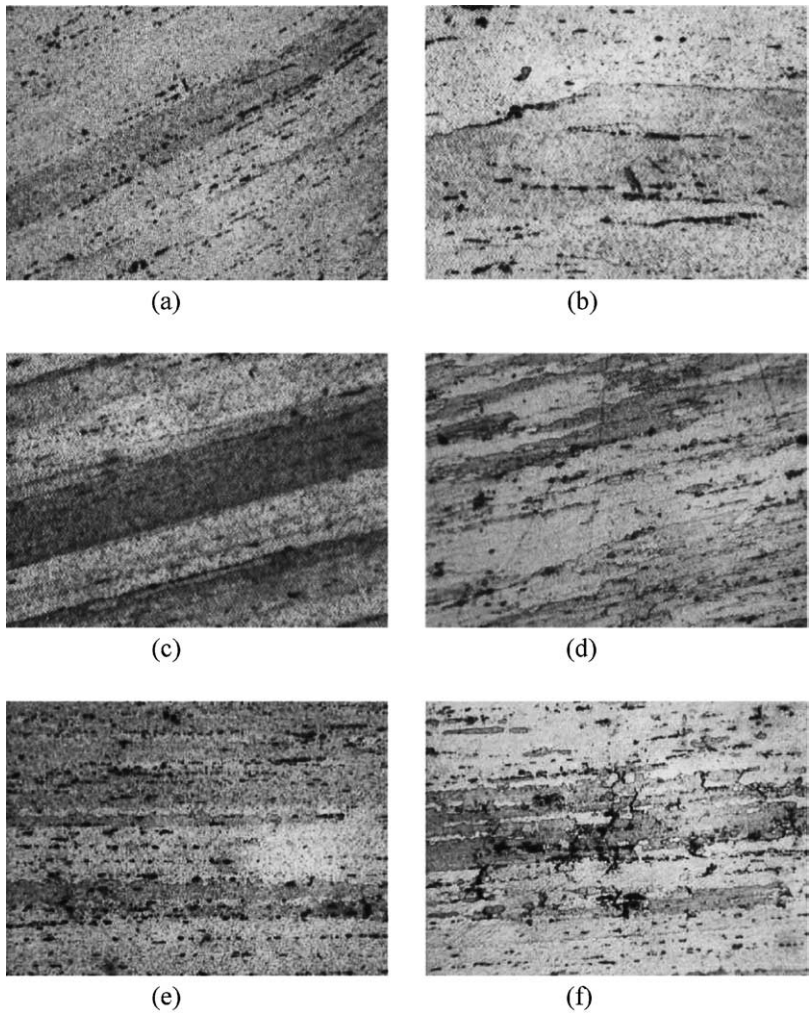

Fig. 11. Metallographs near the fracture portion of tensile specimens undergoing different heating-rate histories (100×). (a) $T_f = 100$ °C, $dT/dt = 200$ °C/s (A-200); (b) $T_f = 100$ °C, $dT/dt = 1000$ °C/s (A-1000); (c) $T_f = 350$ °C, $dT/dt = 200$ °C/s (B-200); (d) $T_f = 350$ °C, $dT/dt = 1000$ °C/s (B-1000); (e) $T_f = 495$ °C, $dT/dt = 200$ °C/s (C-200); (f) $T_f = 495$ °C, $dT/dt = 1000$ °C/s (C-1000).

could be observed that, in general, for a fixed working temperature T_f, more defects can be found in the specimens undergoing higher heating-rate histories. Less defects could be observed in the metallographs corresponding to $T_f = 350$ °C (Fig. 11(c) and (d)). It could be attributed to the adequate recrystallization of the material at this temperature, which eliminated the texture formed during the previous drawing process so that the material could endure more plastic deformation. For $T_f = 495$ °C, more defects (Fig. 11(e) and (f)) can be found, which could be attributed to the more severe thermal stress, material softening, and growth of grains at high temperature. The microstructure shown in Fig. 11 can account for the macroscopic behavior shown in Figs. 2–4. For example, the ductile fracture pattern and the larger contraction ratio of cross section at $T_f = 350$ °C, and the lower rupture strength of specimens heated at higher heating-rate. The latter could also be attributed to LTI, which, together with the applied stress and thermal stress, may bring about more defects (or damage) in the corresponding specimens. As was mentioned previously, at $T_f = 100$ °C,

the rupture strength corresponding to the heating-rate of 600 °C/s is slightly higher than that at heating-rate of 200 and 1000 °C/s. It could be accounted for with the LTI, which causes moderate local residual stress distribution, assisting the hardening of the material. At lower heating-rate, the LTI is not distinct, and at higher heating-rate, the damage caused by severe LTI may become dominant. At both $T = 350$ and 495 °C, the rupture strength decreases with the increase of heating-rate, which could be accounted for with the damage by LTI at higher heating-rate.

3. FE simulation for the mechanism of LTI through a simple example

A simple case was simulated with finite element approach to verify the effect of LTI at different heating-rate. Consider a representative cell, consisting of a small pure aluminum cylinder and a tiny spherical alumina-type inclusion located at the center of the cylinder. When the cell is heated by applying an electrical voltage U between the two ends of the cylinder, the difference between the electrical and thermal properties of the two phases may cause LTI. In computation, both the diameters and the length of the cylinder are taken as 2 mm respectively and the boundary is free. The inclusion sphere has radii of 0.05, 0.1 and 0.2 mm, respectively. The thermal, electrical and mechanical properties of matrix and inclusion materials used for the simulation are shown in Table 5 (Mencik, 1992). The difference in the thermal and electrical properties between phases, such as thermal and electrical conductivity and specific heat, affect the temperature distribution during an electrical heating process. While the mechanical properties, such as elastic modulus, Poisson's ratio and thermal expansion coefficient, affect the local residual thermal stress.

In order to investigate the local residual thermal stress caused by LTI, as an initial simulation and for simplicity, the influence of the difference in thermal expansion coefficients between the matrix and the inclusion materials was temporarily ignored. Assuming the thermal expansion coefficients of the two materials to be identical, i.e., $\alpha_m = \alpha_i = 23 \times 10^{-6}\ K^{-1}$, the contribution from the average part of temperature distribution will be automatically filtered.

Fig. 12(a)–(c) shows respectively the distributions of temperature T, Mises equivalent stress σ_e and pressure p ($p = -\sigma_{kk}/3$) obtained by applying $U = 0.03$ V between the two ends of the cylinder with an inclusion of $r_{inc} = 0.1$ mm for 0.01 s. It can be seen that the final temperature varies between 12.14 and 30.08 °C, the corresponding overall heating-rate is about 3000 K/s. The Mises equivalent stress is defined as follows

$$\sigma_e = \sqrt{\frac{3}{2} s_{ij} s_{ij}}, \quad \text{with} \quad s_{ij} = \sigma_{ij} - \frac{1}{3}\sigma_{kk}\delta_{ij}. \tag{1}$$

It can be seen in Fig. 12(b) that the induced maximum equivalent stress could be as high as 56.62 MPa. It can be imagined that with the increase of heating-rate, the induced additional local residual stress may further increase, which, combined with the existing residual stress and the stress induced by the external

Table 5
Properties of matrix and inclusion materials used in simulation

	Matrix	Inclusion
Density (g/m^3)	2700	3980
Electrical conductivity ((Ω m)$^{-1}$)	3.8×10^7	10^{-12}
Thermal conductivity (W/(m K))	247	1.2
Specific heat (J/(kg K))	917	1000
Young's modulus (GPa)	62	400
Poisson's ratio	0.33	(0.17)
Thermal expansion coefficient (10^{-6}/K)	23	6

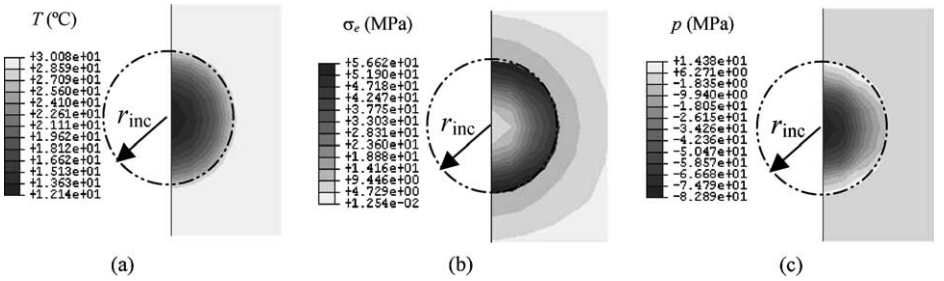

Fig. 12. Distributions of temperature, equivalent stress and volumetric stress at $\dot{T} = 3000$ K/s (with thermal expansion coefficients $\alpha_m = \alpha_i = 23 \times 10^{-6}$ K^{-1}). (a) Distribution of T, (b) distribution of σ_e, (c) distribution of p.

load (for instance, the preloaded stress), may be sufficiently large to cause local damage in the material. On the other hand, the distribution of temperature, as shown in Fig. 12(a), may also result in marked tensile volumetric stress in the inclusion (Fig. 12(c)), which may deteriorate the capability of the material to resist damage.

Fig. 13(a) shows the variation of maximum equivalent stress $\sigma_{e,max}$ against heating-rate, taking inclusion radius r_{inc} as a parameter. It can bee seen that, if r_{inc} is fixed, $\sigma_{e,max}$ increases almost linearly with the increase of heating-rate. The larger the inclusion is, the larger the maximum equivalent stress will be. It can be seen in Fig. 13(b), $\sigma_{e,max}$ increases as r_{inc} increases, but the variation of $\sigma_{e,max}$ with respect to r_{inc} is not linear, the slope decreases as r_{inc} increases. Computation also shows that, for a fixed heating rate, the steady state local residual thermal stress distribution can be achieved at a low level of temperature when the gradient of temperature distribution tends to be stable. Fig. 13(c) shows the variations of $\sigma_{e,max}$, T_{max}, T_{min} and $T_{max} - T_{min}$ in the representative cell with the inclusion of radius 0.1 mm during an electrical heating process. It can be found that both $\sigma_{e,max}$ and $T_{max} - T_{min}$ tend to be stable at $t = 0.02$ s when $T_{max} \approx 60$ °C. It indicates that the LTI induced by high heating-rate may play a significant role in the change as well as the degradation of the mechanical properties of materials even at low temperature.

If the different thermal expansion coefficients of the matrix and inclusion materials is taken into account, i.e., $\alpha_m = 23 \times 10^{-6}$, $\alpha_i = 6 \times 10^{-6}$ were employed, the local residual thermal stress distributions, corresponding to the temperature distribution shown in Fig. 13(a), can be computed and shown in Fig. 14. Compared with the results shown in Fig. 13(b) and (c), marked difference in both the distribution and the magnitude can easily be observed. Computation also shows that, ignoring the effect of temperature on the material properties shown in Table 5 and assuming elastic response, $\sigma_{e,max}$ increases almost linearly with the increase of average temperature, but decreases with the increase of the size of inclusion. If the temperature is very high, the induced local residual thermal stress can also be sufficiently large to cause damage in the material.

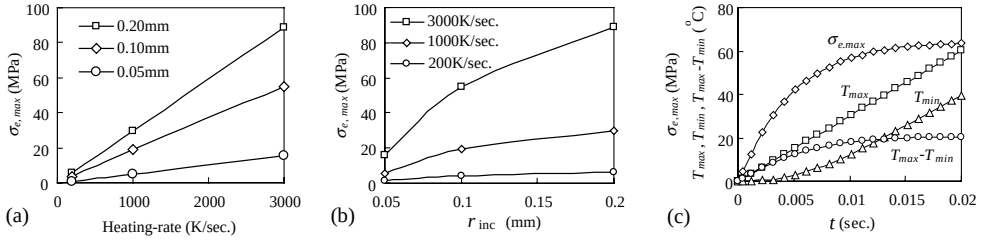

Fig. 13. Variations of maximum residual stress $\sigma_{e,max}$ and temperature T during heating (with thermal expansion coefficients $\alpha_m = \alpha_i = 23 \times 10^{-6}$ K^{-1}). (a) Variation of $\sigma_{e,max}$ vs. heating-rate; (b) variation of $\sigma_{e,max}$ vs. r_{inc}; (c) variations of $\sigma_{e,max}$ and T vs. t.

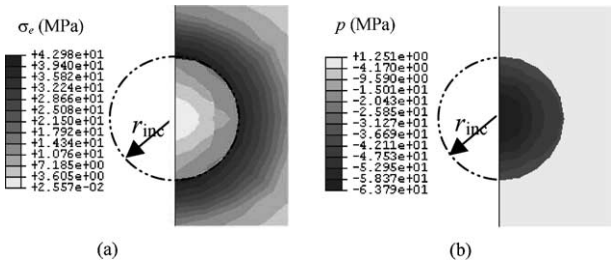

Fig. 14. Distributions of equivalent stress and volumetric stress (with thermal expansion coefficients $\alpha_m = 23 \times 10^{-6}$, $\alpha_i = 6 \times 10^{-6}$). (a) Distribution of σ_e, (b) distribution of p.

4. Discussion and conclusions

Using a Gleeble 1500 thermal–mechanical testing system, two classes of experiments were made to investigate the dependence of tensile rupture strength of aluminum alloy LY12 on heating-rate history and the dependence of the failure temperature of preloaded specimens on heating-rate. The metallographs of the tested material were analyzed and a FE simulation was performed to investigate the mechanisms of heating-rate effect.

At a prescribed working temperature, the rupture strength of LY12, in general, decreases as heating-rate increases. On the other hand, if a preloaded LY12 specimen is heated, the specimen would fail at lower temperature if either heating-rate increases or preloaded stress decreases. For both cases, the analysis to the metallographs of the material near the fracture section of tested specimens showed that defects increase with the increase of heating-rate.

Since a material is substantially heterogeneous, the inhomogeneous nature may cause LTI between different parts of microstructure during a fast-heating process. LTI may further induce additional local residual stress fields and influence the macroscopic mechanical properties of the material. Specifically speaking, moderate heating-rate may help generating LTI and local stress fields, contributing to material hardening. However, severe local residual stress due to the strong LTI at very high heating-rate may cause initiation and growth of damage in the microstructure, resulting in a degradation of the macroscopic mechanical properties of the material.

Recrystallization also strongly affects the material behavior during a fast-heating process, which is related to temperature, heating time interval and applied stress. Recrystallization can eliminate the existing or plastic deformation induced anisotropic microstructure (e.g., texture), and can enhance the endurance of materials to further plastic deformation. However, at very high temperature, the grains may overgrowth, which may degrade the mechanical properties of materials.

The concept of LTI was verified with a numerical example. It shows that, the maximum equivalent local residual thermal stress $\sigma_{e,max}$ increases with the increase of either heating-rate or temperature. For a prescribed heating-rate, $\sigma_{e,max}$ approaches its saturated value at fairly low temperature. Considering the existing stress caused by external thermal–mechanical load, and the existing residual microstress fields, the superposition of the local stress caused by LTI may cause or increase the tendency of material damage. It indicates that the LTI induced by high heating-rate may play a significant role in the change as well as the degradation of the mechanical properties of materials.

The research on the effect of fast heating has also a practical engineering background. For instance, in the fast micropart stamping process assisted with electrical heating, the shearing zone of the work material should be heated to a favorite stamping temperature in a very short time interval to meet the requirement of mass production (Strathclyde University, 2000). For aluminum, if the favorite stamping temperature for aluminum is 400 °C and the heating time interval is limited within 40 ms, the heating-rate can be as high as

10,000 K/s. From the above analysis, it can be seen that the effect of heating-rate should be considered if a high accurate micropart stamping process is simulated.

References

Chen, B., Peng, X., et al., 2001. An experimental investigation to the effect of heating rate on the failure of pre-load H62 brass. Acta Metallurgica Sinica 37 (12), 1256–1260.

Chen, H. et al., 1992. Thermomechanical response of Al plates under tension to CW CO_2 laser radiation. High Power Laser and Particle Beams 4 (1), 141–147.

Chen, Y., 1997. Progress in structural mechanics in the Academy of Engineering Physics of China. In: Zhuang, F. (Ed.), Modern Mechanics and Progresses in Science and Technology. Tsinghua University Press, Beijing, pp. 329–335.

Chen, Y., Li, S., 1992. Buckling failure of the axially precompressed cylindrical shell irradiated by CW CO_2 laser beam. AIAA, 92–3231.

Chen, Y., Li, G., Zhang, J., 1995. Transient fatigue of aluminum plate in tension and irradiated by CW CO_2 laser beam. High Power Laser and Particle Beams 7 (2), 245–251.

Han, M., Liu, Z., Liu, Y., 1999. An experimental study on the mechanical behavior of A_3 steel under rapid heating. Explosion and Impact 19 (1), 20–26.

Li, S., Chen, Y., 1994. Failure of shell subjected to internal pressure and irradiated by CW CO_2 laser beam. AIAA, 94–2461.

Liu, Z., Han, M., Sun, C., Wang, R., 1995. Inelastic thermo-softening of metals under rapid heating. Acta Metallurgica Sinica 31 (7), B229–335.

Liu, Z., Feng, Z., et al., 1996. Studies of thermo-softening of three alloys under short-time elevated temperature. Explosion and Impact 16 (2), 98–104.

Mencik, J., 1992. Strength and Fracture of Glass and Ceramics. Elsevier.

University of Strathclyde et al., 2000. Tool technology for high accuracy micro-part stamping (TOPAS), Mid-Term Report, BRPR-CT98-0742, EU Brite-EuRam Project Report.

Wang, C., Huang, C., Sun, Y., Duan, Z., 1995. Influence of heating rate and strain rate on tensile strength of 30CrMnSi. Acta Metallurgica Sinica 31 (10), A475–478.